ELSEVIER

Journal of Organometallic Chemistry 517 (1996) 217–226

Journal of Organometallic Chemistry

Rhenium carbonyls containing pyridyl ligands incorporating an alkyne entity

Jiann T. Lin [a,*], Shih-Sheng Sun [a], Jiann Jung Wu [a], Yen-Chywan Liaw [b], Kuan-Jiuh Lin [a]

[a] *Institute of Chemistry, Academia Sinica, Nankang, Taipei, Taiwan*
[b] *Institute of Biomedical Science, Academia Sinica, Nankang, Taipei, Taiwan*

Received 6 December 1995; in revised form 24 January 1996

Abstract

Reactions of pyridyl ligands, 4,4′-dipyridylbutadiyne (DPB), 1,4-bis(4′-pyridylethynyl)benzene (BPEB), ferrocenyl-4-pyridylacetylene (FPA), 4-nitrophenyl-4′-pyridylacetylene (NPPA) and 4-aminophenyl-4′-pyridylacetylene (APPA), with $Re(CO)_5X$ (X = Cl,Br), *cis*-$Re(CO)_4(L)Cl$ (L = PPh_3, $P(OMe)_3$), and $[Re(CO)_3(2,2'\text{-bipy})(MeCN)][PF_6]$, provides *fac*-$Re(CO)_3(\eta^1\text{-DPB})_2Cl$ (**1**), *fac*-$Re(CO)_3(PY)_2Br$ (**2**, PY = FPA; **3**, L = NPPA; **4**, L = APPA), $[fac\text{-}Re(CO)_3(PPh_3)Cl]_2(\mu\text{-PY})$ (**5**, PY = BPEB; **6**, PY = DPB), $[fac\text{-}Re(CO)_3(P(OMe)_3)Cl]_2(\mu\text{-DPB})$ (**7**), *fac*-$Re(CO)_3(PPh_3)(PY)Cl$ (**8**, PY = NPPA; **9**, PY = FPA), $[fac\text{-}Re(CO)_3(2,2'\text{-bipy})(PY)][PF_6]$ (**10**, PY = NPPA; **11**, PY = APPA; **12**, PY = FPA), and $[\{fac\text{-}Re(CO)_3(2,2'\text{-bipy})\}_2(\mu\text{-PY})][PF_6]_2$ (**13**, PY = DPB; **14**, PY = BPEB). The energy of the metal to pyridyl π^* charge-transfer (MLCT) is investigated by electronic absorption spectra and cyclic voltammetry. X-ray structural analyses for **2** · CH_2Cl_2 and **12** · $2H_2O$ were carried out. **2** · CH_2Cl_2: $C_{12}H_{28}BrClN_2O_3P_2Fe_2Re$; monoclinic; $P2_1/n$, $Z = 4$; $a = 15.188(2)$, $b = 15.100(2)$, $c = 16.254(1)$ Å; $\beta = 102.22(1)°$; $R = 0.047$; $Rw = 0.040$. **12** · $2H_2O$: $C_{30}H_{21}F_6N_3O_3PFeRe$; monoclinic; $P2_1/n$, $Z = 4$; $a = 19.022(4)$, $b = 9.339(2)$, $c = 21.111(3)$ Å; $\beta = 116.156(9)°$; $R = 0.043$; $Rw = 0.061$.

Keywords: Rhenium; Alkyne; Pyridene; Carbonyl

1. Introduction

Organometallic nonlinear optical materials have attracted considerable interest recently [1]. Our interest in this area led us to synthesize several pyridyl ligands incorporating an alkyne entity, as well as tungsten carbonyl complexes derived from these ligands [2]. The metal fragment in metal pyridyl complexes could function as an electron-donor [3] owing to the presence of the strong metal to ligand charger transfer (MLCT) normally present in pyridyl metal complexes [4], or as an electron-acceptor based on the σ-donating from the nitrogen atom to metal center [5]. Furthermore, the presence of carbonyl ligands should offer the opportunity for tuning the metal environment electronically and sterically via ligand substitution. Juxtaposition of the alkyne entity and ligands might also have applications in other aspects: (a) two or more metal centers could be held in the same molecule [6] for cooperative effect in catalysis; (b) metal organic polymers could be derived from organometallic complexes containing these ligands [7]; (c) bridged dinuclear complexes could serve as models for the investigation of metal–metal interactions [8].

Since our first report on dinuclear tungsten carbonyls bridged by conjugated pyridyl ligands, our continual efforts are to vary metal moieties as well as pyridyl ligands in these systems. In this report, we will describe the syntheses and structural and spectroscopic studies of some rhenium carbonyl complexes which contain pyridyl ligands reported in Ref. [2].

2. Experimental section

2.1. Materials and apparatus

The ^1H and ^{31}P NMR spectra were recorded on Bruker AC200 or AC300 spectrometers. IR spectra were measured with a Perkin–Elmer 880 spectrometer. Mass spectra (FAB) were recorded on a VG70-250S

* Corresponding author. Fax: 886-2-7831237; e-mail: jtlin@chem.sinica.edu.tw.

PII S0022-328X(96)06167-0

mass spectrometer. Elementary analyses were performed on a Perkin–Elmer 2400 CHN analyzer. Electronic absorption spectra were obtained on a Perkin–Elmer Lambda 9 spectrometer. Electrochemical measurements were recorded on a Bioanalytical System BAS 100B. Cyclic voltammograms were obtained in deoxygenated dry CH_2Cl_2 or CH_3CN with a platinum working electrode, a platinum wire auxiliary electrode, and a saturated $Ag–AgNO_3$ reference electrode with 0.1 M tetrabutylammonium perchlorate (TBAP) as supporting electrolyte. In some cases, ferrocene, which was known to undergo a discrete one-electron transfer process, was added and used as internal reference for both the potential calibration and for reversibility criteria. In CH_2Cl_2 the ferrocene has $E_{1/2}$ at 0.223 V relative to $Ag–Ag^+$ and the anionic peak-cathodic peak separation is 105 mV. All E_p values for the complexes in this study are reported relative to ferrocene (i.e. 0.00 V for ferrocene). The concentration of the metal carbonyls in these measurements was ca. 10^{-3} M. The scan rate was 80 mV s^{-1}. The measurements were uncorrected for liquid-junction potentials.

All reactions and manipulations were carried out under N_2 with use of standard inert-atmosphere and Schlenk techniques. Solvents were dried by standard procedures. All column chromatography was performed under N_2 with use of silica gel (230–400 mesh ASTM, Merck) as the stationary phase in a column 35 cm in length and 2.5 cm in diameter. $Re(CO)_5X$ (X = Cl, Br) [9], *cis*-$Re(CO)_4(L)Cl$ (L = PPh_3, $P(OMe)_3$) [10], $[(Re(CO)_3(2,2'\text{-bipy})(MeCN)][PF_6]$ [11], ferrocenyl-4-pyridylacetylene (FPA), 4,4'-dipyridylbutadiyne (DPB), 1,4-bis(4'-pyridylethynyl)benzene (BPEB), 4-nitrophenyl-4'-pyridylacetylene (NPPA), and 4-aminophenyl-4'-pyridylacetylene (APPA), were prepared by published procedures [2].

2.2. *fac-Re(CO)$_3$(η^1-DPB)$_2$Cl (1)*

A solution of $Re(CO)_5Cl$ (200 mg, 0.55 mmol) in CH_2Cl_2 (15 ml) was added over a 4 h period to a refluxing solution of DPB (250 mg, 1.23 mmol) in 100 ml of benzene. The resulting solution was refluxed for an additional 4 h and the solvent was removed in vacuo. The residue was recrystallized from CH_2Cl_2–hexane to provide the bright yellow powdery **1** in 83% yield (326 mg). MS (FAB): *m/e* 715 ($(M+1)^+$, ^{185}Re). Anal. Found: C, 52.01; H, 1.99; N, 7.64. $C_{31}H_{16}ClN_4O_3Re$. Calc.: C, 52.14; H, 2.26; N, 7.85%.

2.3. *fac-Re(CO)$_3$(PY)$_2$Br (2, PY = FPA; 3, PY = NPPA; 4, PY = APPA)*

Essentially the same procedures were followed for the syntheses of **2–4**, and only the preparation of **2** will be described in detail. A benzene solution (70 ml) containing $Re(CO)_5Br$ (130 mg, 0.32 mmol) and FPA (200 mg, 0.70 mmol) was refluxed in the dark for 16 h. After removal of the solvent, the crude product was triturated with hexane and washed with Et_2O (3 × 50 ml) to provide red powdery **2** in 88% yield (180 mg). MS (FAB): 924 ($(M+1)^+$, ^{185}Re). Anal. Found: C, 47.73; H, 2.89; N, 2.66. $C_{37}H_{26}BrFe_2N_2O_3Re$. Calc.: C, 48.05; H, 2.81; N, 3.03%.

Yellow orange complex **3** was isolated in 82% yield. Anal. Found: C, 43.72; H, 1.91; N, 6.74. $C_{29}H_{16}BrN_4O_7Re$. Calc.: C, 43.60; H, 2.00; N, 7.02%.

Yellow complex **4** was isolated in 37% yield. MS (FAB): *m/e* 738 ($(M+1)^+$, ^{185}Re). Anal. Found: C, 46.86; H, 2.93; N, 7.39. $C_{29}H_{20}BrN_4O_3Re$. Calc.: C, 47.15; H, 2.80; N, 7.59%.

2.4. *[fac-Re(CO)$_3$(L)Cl]$_2$(μ-PY) (5, L = PPh$_3$, PY = BPEB; 6, L = PPh$_3$, PY = DPB; 7, L = P(OMe)$_3$, PY = DPB)*

Essentially the same procedures were followed for the syntheses of **5–7**, and only the preparation of **5** will be described. A benzene solution (80 ml) containing *cis*-$Re(CO)_4(PPh_3)Cl$ (1.00 g, 1.68 mmol) and BPEB (250 mg, 0.89 mmol) was refluxed in the dark for 16 h. The solution was concentrated to ca. 40 ml and the slow addition of hexane (50 ml) led to the precipitation of orange-yellow solid, which was chromatographed on silica gel. Elution with CH_2Cl_2–hexane (1 : 1) gave **5** (270 mg, 21%) as a yellow solid. MS (FAB): *m/e* 1414 (M^+, ^{185}Re). Anal. Found: C, 52.11; H, 3.02; N, 2.14. $C_{62}H_{42}Cl_2N_2O_6P_2Re_2$. Calc.: C, 52.55; H, 2.99; N, 1.98%.

Deep yellow complex **6** was eluted with CH_2Cl_2–hexane (3 : 2). Yield: 29%. MS (FAB): *m/e* 1337 (M^+, ^{185}Re). Anal. Found: C, 49.55; H, 3.10; N, 1.89. $C_{56}H_{38}Cl_2N_2O_6P_2Re_2$. Calc.: C, 50.19; H, 2.86; N, 2.09%.

Yellow complex **7** was eluted with CH_2Cl_2. Yield: 33%. MS (FAB): *m/e* 1065 ($(M+1)^+$, ^{185}Re). Anal. Found: C, 29.69; H, 2.38; N, 2.61. $C_{26}H_{26}Cl_2N_2O_{12}P_2Re_2$. Calc.: C, 29.89; H, 2.49; N, 2.68%.

2.5. *fac-Re(CO)$_3$(PPh$_3$)(PY)Cl (8, PY = NPPA; 9, PY = FPA)*

The preparation of **8** or **9** is similar to the procedure described for **6** except that an equimolar quantity of PY was used. Deep yellow powdery **8** was obtained in 33% yield. MS (FAB): *m/e* 794 (M^+, ^{187}Re). Anal. Found: C, 51.29; H, 2.69; N, 3.54. $C_{34}H_{23}ClN_2O_5PRe$. Calc.: C, 51.52; H, 2.90; N, 3.54%. Orange powdery **9** was obtained in 46% yield. MS (FAB): *m/e* 821 ($(M+1-Cl)^+$, ^{187}Re). Anal. Found: C, 53.16; H, 3.12; N, 1.32. $C_{38}H_{28}ClFeNO_3PRe$. Calc.: C, 53.36; H, 3.28; N, 1.64%.

2.6. [fac-Re(CO)$_3$(2,2'-bipy)(PY)][PF$_6$] (10, PY = NPPA; 11, PY = APPA; 12, PY = FPA)

Essentially the same procedures were followed for the syntheses of **10–12**, and only the preparation of **10** will be described. A THF solution (150 ml) containing [Re(CO)$_3$(2,2'-bipy)(MeCN)][PF$_6$] (400 mg, 0.66 mmol) and NPPA (190 mg, 0.85 mmol) was refluxed at 80°C in the dark for 5 h. The solvent was removed in vacuo and the residue was washed with Et_2O to afford yellow-orange powdery **10** in a yield of 72% (380 mg). MS (FAB): *m/e* 796 (M^+, ^{187}Re). Anal. Found: C, 39.27; H, 2.13; N, 6.70. $C_{26}H_{16}F_6N_4O_5PRe$. Calc.: C, 39.24; H, 2.01; N, 7.04%.

Orange-red complex **11** was isolated from column chromatography using THF–CH_2Cl_2 (1:9) as eluent. Yield: 50%. Anal. Found: C, 40.86; H, 2.16; N, 7.60. $C_{26}H_{18}F_6N_4O_3PRe$. Calc.: C, 40.78; H, 2.37; N, 7.32%.

Orange-yellow complex **12** was obtained in 89% yield. Anal. Found: C, 42.23; H, 2.33; N, 4.58. $C_{30}H_{21}F_6FeN_3O_3PRe$. Calc.: C, 41.96; H, 2.45; N, 4.90%.

2.7. [{fac-Re(CO)$_3$(2,2'-bipy)}$_2$(μ-DPB)][PF$_6$]$_2$ (13)

A mixture of [Re(CO)$_3$(2,2'-bipy)(MeCN)][PF$_6$] (400 mg, 0.66 mmol) and DPB (70 mg, 0.34 mmol) in THF (100 ml) was refluxed at 70°C in the dark for 2 h. The yellow precipitate was washed with THF (3 × 50 ml) to afford **13** in 30% yield (260 mg). Anal. Found: C, 35.43; H, 1.96; N, 5.99. $C_{40}H_{24}F_{12}N_6O_6P_2Re_2$. Calc.: C, 35.65; H, 1.78; N, 6.24%.

2.8. [{fac-Re(CO)$_3$(2,2'-bipy)}$_2$(μ-BPEB)][PF$_6$]$_2$ (14)

Complex **14** was synthesized by the same procedure as for the synthesis of **13** except that the crude product was further dissolved in MeCN and filtered through Celite. Removal of the solvent and trituration of the residue with Et_2O (20 ml) gave **14** as orange-yellow powders (55%). Anal. Found: C, 39.22; H, 1.90; N, 5.79. $C_{46}H_{28}F_{12}N_6O_6P_2Re_2$. Calc.: C, 38.81; H, 1.97; N, 5.91%.

2.9. Crystallographic studies

Crystals of **2** · CH_2Cl_2 and **12** · $2H_2O$ were grown by slow diffusion of hexane into a concentrated solution of relevant complexes in CH_2Cl_2. Diffraction measurements were made on an Enraf–Nonious CAD4 diffractometer with the θ–2θ scan mode. Unit cells were determined by centering 25 reflections in the suitable 2θ range. Other relevant experimental details are listed in Table 1. All data reduction and refinements were car-

Table 1
Crystal data for compounds **2** · CH_2Cl_2 and **12** · H_2O

	2 · CH_2Cl_2	**12** · $2H_2O$
Formula	$C_{38}H_{28}BrCl_2N_2O_3Fe_2Re$	$C_{30}H_{25}F_6N_3O_5PFeRe$
Formula weight	1009.35	894.55
Crystal size (mm^3)	0.10 × 0.10 × 0.25	0.16 × 0.16 × 0.20
Crystal system	monoclinic	monoclinic
Space group	$P2_1/n$	$P2_1/n$
a (Å)	15.188(2)	19.022(4)
b (Å)	15.100(2)	9.339(2)
c (Å)	16.254(1)	21.111(3)
β (deg)	102.22(1)	116.156(9)
V (Å^3)	3643.2(7)	3366(1)
Z	4	4
D_{calc} (g cm^{-3})	1.840	1.765
F(000)	1960	1744
Radiation	Mo K α (λ = 0.7107 Å)	Mo K α (λ = 0.7107 Å)
μ (cm^{-1})	52.7	41.7
Transmission factors (maximum–minimum)	1.00–0.67	1.00–0.56
2θ range (deg)	2.0–45	2.0–45
Octants	$\pm h(-16-15)$ $+k(0-16)$ $+l(0-17)$	$\sim h(-20-18)$ $+k(0-10)$ $+l(0-22)$
Number of unique reflections	4743	4377
Number of reflections with $I > n\sigma$	3013 (n = 2.5)	2682 (n = 2.0)
Number of variables	421	423
R [a], R_w [b]	0.047, 0.040	0.043, 0.061
Goodness of fit [c]	1.63	2.87
Maximum Δ/σ	0.077	0.048

[a] $R = \Sigma \| F_0 \| - \| F_c \| / \Sigma | F_0 |$. [b] $Rw = [\Sigma w(| F_0 | - | F_c |)^2 / \Sigma w | F_0 |^2]^{1/2}$; $w = 1/[\sigma^2(F_0) + kF_0^2]$. For **2** · CH_2Cl_2, k = 0.00005; for **12** · $2H_2O$, k = 0.0001. [c] Goodness of fit, $S = [(\Sigma w(| F_0 | - | F_c |)^2 / N_{obs} - N_{var})]^{1/2}$; N_{obs} = no. of observed reflections, N_{var} = no. of variables.

ried out on a MicroVax 3800 computer using NRCVAX [12] programs. Intensities were collected and corrected for decay, absorption (empirical, Psi-scan) and Lp effects. The structures were solved using a combination of direct methods [13] and difference Fourier methods and refined by full-matrix least squares techniques. The Br and C3–O3 ligands in $2 \cdot CH_2Cl_2$ were found to be disordered and with a 40% occupancy for each. The

Table 2
Atomic coordinates for $2 \cdot CH_2Cl_2$

Atom	x	y	z	B_{iso} (Å^2)
Re	0.27465(4)	0.05442(4)	0.13547(4)	3.31(3)
Fe1	0.94144(14)	−0.05836(16)	0.27554(12)	4.06(11)
Fe2	0.10346(17)	0.69917(15)	−0.06425(15)	4.86(13)
Br	0.30123	0.00435	−0.00692	4.89(10)
O1	0.0740(8)	0.0186(9)	0.0753(8)	7.7(7)
O2	0.2875(10)	−0.1380(8)	0.1919(8)	8.3(9)
O3	0.24006	0.13618	0.29831	11.9(13)
C1	0.1498(12)	0.0348(9)	0.0976(9)	4.4(9)
C2	0.2859(12)	−0.0648(13)	0.1717(10)	5.4(10)
C3	0.24904	0.08744	0.24800	2.6(7)
C4	0.4617(10)	0.0628(10)	0.2599(8)	3.8(8)
C5	0.5527(10)	0.0662(10)	0.2879(8)	4.1(8)
C6	0.6092(9)	0.0808(8)	0.2320(9)	3.1(7)
C7	0.5661(11)	0.1015(10)	0.1503(9)	4.0(8)
C8	0.4740(11)	0.0990(10)	0.1262(9)	4.0(8)
C9	0.7058(11)	0.0781(9)	0.2595(10)	4.0(8)
C10	0.7832(11)	0.0664(10)	0.2799(9)	3.9(8)
C11	0.8799(10)	0.0512(11)	0.3066(9)	4.2(9)
C12	0.9454(13)	0.0745(11)	0.2638(13)	6.8(12)
C13	1.0285(11)	0.0428(13)	0.3123(14)	6.4(11)
C14	1.0119(14)	−0.0015(15)	0.3837(12)	7.5(12)
C15	0.9173(12)	0.0040(12)	0.3813(9)	5.8(10)
C16	0.8446(14)	−0.1333(17)	0.1994(16)	8.3(15)
C17	0.9177(18)	−0.1096(15)	0.1590(11)	7.8(13)
C18	0.9999(14)	−0.1433(16)	0.2055(14)	7.2(13)
C19	0.9800(15)	−0.1893(13)	0.2724(15)	7.4(14)
C20	0.8853(16)	−0.1817(13)	0.2694(16)	7.6(16)
C21	0.2843(11)	0.2643(9)	0.1442(8)	3.7(8)
C22	0.2770(12)	0.3515(9)	0.1171(9)	4.9(9)
C23	0.2437(9)	0.3699(10)	0.0347(10)	3.5(8)
C24	0.2234(13)	0.3004(11)	−0.0187(9)	5.7(11)
C25	0.2345(13)	0.2146(10)	0.0128(10)	5.7(11)
C26	0.2340(10)	0.4588(12)	0.0064(9)	4.5(9)
C27	0.2233(10)	0.5334(11)	−0.0191(9)	4.1(8)
C28	0.2146(11)	0.6234(10)	−0.0510(10)	4.2(9)
C29	0.1855(11)	0.6452(10)	−0.1362(10)	5.2(9)
C30	0.1844(13)	0.7400(12)	−0.1516(13)	6.4(12)
C31	0.2165(13)	0.7729(11)	−0.0605(16)	7.6(14)
C32	0.2338(12)	0.7022(12)	−0.0048(11)	5.6(10)
C33	−0.0258(16)	0.658(3)	−0.1069(20)	10.7(20)
C34	0.0085(22)	0.6314(18)	−0.022(3)	11.6(27)
C35	0.0325(19)	0.703(3)	0.0271(17)	10.9(19)
C36	0.0128(17)	0.7766(14)	−0.0232(19)	8.1(15)
C37	−0.0221(12)	0.7500(16)	−0.1027(16)	6.0(13)
N1	0.4195(7)	0.0784(7)	0.1791(7)	3.1(6)
N2	0.2661(7)	0.1949(7)	0.0941(7)	3.1(6)
Cl1	1.0045(8)	0.2199(5)	0.4855(5)	17.3(8)
Cl2	0.9623(10)	0.3518(7)	0.3711(6)	23.8(11)
C	1.018(3)	0.268(3)	0.4012(16)	22.9(33)
Br	0.30123	0.00435	−0.00692	4.89
O3	0.24006	0.13618	0.29831	12
C3	0.24904	0.08744	0.24800	2.6
Br′	0.25172	0.10522	0.28088	4.50
C3′	0.28855	0.01115	0.03178	6.0
O3′	0.31598	−0.00045	−0.04042	9.6

oxygen atom (O5) in one of the H_2O molecules in **12** · $2H_2O$ was also disordered with a 50% occupancy. Except for Br, Br′, C3, C3′, O3, and O3′ atoms in **2**, all non-hydrogen atoms were refined anisotropically. All hydrogen atoms were included in the structure factor calculation in idealized positions with $d_{C-H} = 0.95$ Å. The final positional parameters are listed in Tables 2 and 3, and selected interatomic distances and bond angles are given in Table 4.

3. Results and discussion

Previously we synthesized [2] tungsten carbonyls containing pyridyl ligands, BPEB, DPB, FPA, NPPA, and APPA. We have now extended our studies to rhenium complexes. In accordance with literature reports for the syntheses of *fac*-$Re(CO)_3(L)(L')X$ (L, L′: N or P donor ligands) [14], thermal reactions of $Re(CO)_5X$ (X = Cl, Br) and *cis*-$Re(CO)_4(L)Cl$, (L =

Table 3
Atomic coordinates for **12** · $2H_2O$

Atom	x	y	z	B_{iso} (Å^2)
Re	0.22818(4)	0.2505(1)	0.14081(3)	3.40(4)
Fe	0.3542(2)	−0.0446(4)	−0.2682(2)	6.2(2)
P	0.0446(3)	−0.0790(6)	0.8556(3)	5.7(3)
F1	0.035(2)	−0.081(2)	0.7839(9)	19(2)
F2	0.057(1)	−0.077(2)	0.9327(8)	19(2)
F3	0.0052(9)	−0.230(2)	0.843(1)	16(1)
F4	0.0847(7)	0.072(1)	0.8731(6)	8.6(8)
F5	−0.0343(8)	−0.0088(20)	0.832(1)	16(2)
F6	0.1246(8)	−0.151(2)	0.886(1)	15(1)
O1	0.1714(7)	−0.057(1)	0.1450(7)	6.2(9)
O2	0.3747(7)	0.188(1)	0.2759(6)	6.2(8)
O3	0.1534(8)	0.366(1)	0.2317(6)	5.8(8)
N1	0.2811(7)	0.181(2)	0.0709(6)	3.7(8)
N2	0.2608(7)	0.466(1)	0.1252(6)	3.4(8)
N3	0.1298(7)	0.325(2)	0.0444(6)	3.7(7)
C1	0.192(1)	0.060(2)	0.1443(8)	4.3(10)
C2	0.320(1)	0.208(2)	0.2251(8)	4.5(11)
C3	0.182(1)	0.321(2)	0.1992(8)	4.0(10)
C4	0.2407(9)	0.103(2)	0.0141(9)	4.3(10)
C5	0.270(1)	0.056(2)	−0.0317(9)	4.8(11)
C6	0.348(1)	0.091(2)	−0.0196(9)	4.7(11)
C7	0.388(1)	0.174(3)	0.039(1)	7.6(15)
C8	0.355(1)	0.214(2)	0.0843(9)	6.0(13)
C9	0.375(1)	0.046(3)	−0.067(1)	6.0(13)
C10	0.393(1)	0.013(2)	−0.1092(9)	5.1(12)
C11	0.420(1)	−0.035(2)	−0.159(1)	6.7(15)
C12	0.417(1)	−0.176(3)	−0.183(1)	7.9(16)
C13	0.449(2)	−0.170(3)	−0.233(1)	11(2)
C14	0.471(1)	−0.033(3)	−0.0239(1)	9.7(20)
C15	0.453(1)	0.051(3)	−0.193(1)	8.2(17)
C16	0.267(1)	0.103(3)	−0.315(1)	9.3(17)
C17	0.240(1)	−0.018(3)	−0.293(1)	11(2)
C18	0.247(2)	−0.142(3)	−0.331(1)	11(2)
C19	0.281(2)	−0.097(3)	−0.371(1)	9.5(20)
C20	0.294(1)	0.044(3)	−0.365(1)	8.7(18)
C21	0.328(1)	0.532(2)	0.1672(8)	4.4(10)
C22	0.348(1)	0.664(2)	0.1541(9)	5.0(11)
C23	0.297(1)	0.733(2)	0.097(1)	5.8(12)
C24	0.226(1)	0.670(2)	0.0516(9)	5.1(11)
C25	0.2097(9)	0.537(2)	0.0651(8)	3.7(10)
C26	0.1365(9)	0.461(2)	0.0212(8)	3.3(9)
C27	0.078(1)	0.514(2)	−0.0395(8)	4.3(10)
C28	0.013(1)	0.434(2)	−0.0772(9)	5.1(11)
C29	0.0057(10)	0.300(2)	−0.0534(9)	4.7(10)
C30	0.0649(9)	0.251(2)	0.0075(8)	4.4(10)
O4	0.4971(7)	0.5379(16)	0.1051(7)	6.8(9)
O5	0.4246(12)	0.7253(25)	0.0000(11)	4.4(5)
O5′	0.3894(14)	0.617(3)	−0.0125(13)	5.4(6)

Table 4
Selected bond distances (Å) and angles (deg) for $2 \cdot CH_2Cl_2$ and $12 \cdot 2H_2O$

	2	12
Re–Br; Re–Br′	2.55; 2.58	
Re–N1	2.19(1)	2.22(1)
Re–N2	2.22(1)	2.18(1)
Re–N3		2.18(1)
Re–C1	1.89(2)	1.92(2)
Re–C2	1.89(2)	1.90(2)
Re–C3; Re–C3′	2.01; 1.86	1.92(2)
Fe or Fe1–C11; Fe2–C28	2.03(2); 2.01(2)	2.08(2)
Fe or Fe1–C12; Fe2–C29	2.02(2); 2.05(2)	2.07(2)
Fe or Fe1–C13; Fe2–C30	2.03(2); 2.03(2)	2.00(2)
Fe or Fe1–C14; Fe2–C31	2.04(2); 2.04(2)	2.04(2)
Fe or Fe1–C15; Fe2–C32	2.06(2); 2.01(2)	2.06(2)
Fe or Fe1–C16; Fe2–C33	2.05(2); 2.04(2)	2.05(2)
Fe or Fe1–C17; Fe2–C34	2.01(2); 2.01(3)	2.02(2)
Fe or Fe1–C18; Fe2–C35	2.04(2); 2.01(2)	2.09(3)
Fe or Fe1–C19; Fe2–C36	2.06(2); 2.02(2)	2.06(2)
Fe or Fe1–C20; Fe2–C37	2.04(2); 2.03(2)	2.02(2)
C1–O1	1.16(2)	1.17(2)
C2–O2	1.15(2)	1.14(2)
C3–O3; C3′–O3′	1.13; 1.34	1.12(2)
N1–C4; N1–C8	1.35(2); 1.35(2)	1.32(2); 1.34(2)
N2–C21; N2–C25	1.32(2); 1.34(2)	1.34(2); 1.38(2)
N3–C26; N3–C30		1.39(2); 1.33(2)
C9–C10; C26–C27	1.16(2); 1.20(2)	1.13(2)
C1–Re–C2	88.3(7)	88.1(7)
C1–Re–C3; C1–Re–C3′	87.7; 87.1	91.2(7)
C1–Re–Br; C1–Re–Br′	89.9; 91.4	
C1–Re–N1	179.5(5)	91.5(6)
C1–Re–N2	93.5(5)	174.0(6)
C1–Re–N3		99.2(6)
C2–Re–C3; C2–Re–C3′	88.6; 85.9	87.7(7)
C2–Re–Br; C2–Re–Br′	88.8; 91.1	
C2–Re–N1	92.2(6)	93.8(6)
C2–Re–N2	178.2(6)	97.4(6)
C2–Re–N3		172.7(6)
C3–Re–Br; C3′–Re–Br′	176.55; 176.57	
C3–Re–N1; C3′–Re–N1	92.2; 93.0	176.9(6)
C3–Re–N2; C3′–Re–N2	91.6; 94.1	91.3(6)
C3–Re–N3		92.3(6)
Br–Re–N1; Br′–Re–N1	90.1; 88.6	
Br–Re–N2; Br′–Re–N2	91.1; 89.0	
N1–Re–N2	86.0(4)	85.8(5)
N1–Re–N3		85.8(5)
Re–C1–O1	177(1)	178(2)
Re–C2–O2	176(2)	178(2)
Re–C3–O3; Re–C3′–O3′	153.62; 163.12	177(2)
C6–C9–C10	173(2)	175(2)
C9–C10–C11	179(2)	176(2)
C23–C26–C27	178(2)	
C26–C27–C28	177(2)	

PPh_3, $P(OMe)_3$), with appropriate pyridines provide complexes *fac*-$Re(CO)_3(\eta^1\text{-DPB})_2Cl$ (**1**), *fac*-$Re(CO)_3(PY)_2Br$ (**2** PY = FPA; **3**, L = NPPA; **4**, L = APPA), [*fac*-$Re(CO)_3(PPh_3)Cl]_2(\mu\text{-PY})$ (**5**, PY = BPEB; **6**, PY = DPB), [*fac*-$Re(CO)_3(P(OMe)_3)Cl]_2(\mu\text{-DPB})$ (**7**), and *fac*-$Re(CO)_3(PPh_3)(PY)Cl$ (**8**, PY = NPPA; **9**, PY = FPA). Cationic complexes, [*fac*-$Re(CO)_3$(2,2′-bipy)(PY)][PF_6] (**10**, PY = NPPA; **11**, PY = APPA; **12**, PY = FPA), [{*fac*-$Re(CO)_3$(2,2′-bipy)}$_2(\mu\text{-PY})$][PF_6]$_2$ (**13**, PY = DPB; **14**, PY = BPEB), could also be synthesized from [$(Re(CO)_3$(2,2′-bipy)(MeCN)][PF_6]. The IR and ^1H NMR data for all these complexes are summarized in Table 5. Three strong carbonyl bands in the infrared spectra are consistent with the facial disposition of the three carbonyl ligands in these complexes. The α-ring protons of pyridines for the complexes **1–9** have chemical shifts which appear at lower field than those of free ligands [2] in the ^1H NMR spectra. The lower δ values for the α-ring protons of pyridine in **10–14** are probably due to the ring current shielding caused by the bipy ligands.

The metal (rhenium) to π^* (pyridine) charge-transfer (MLCT) absorption spectra of all new complexes in CH_2Cl_2 and CH_3CN are shown in Table 6. For complexes **5–9**, a good correlation (supplementary materials) exists between the MCLT bands and the solvent parameter, E^*_{MLCT} (defined between 0.00 (isooctane) and 1.00 (dimethyl sulfoxide)) [15]. These MLCT transitions bands (320–395 nm) appear at shorter wavelengths than those (390–600 nm) in $W(CO)_4(L)(PY)$ and $[W(CO)_4(L)]_2(\mu\text{-PY}')$ (L = CO, phosphine, phosphite; PY, PY′ = DPB, BPEB, FPA, NPPA, APPA) [2], and exhibit only minor blue shift as the solvent polarity increases. This phenomenon is similar to that found in *fac*-$ClRe(CO)_3(L)_2$ (L = 4-phenylpyridine, 4,4′-bipyridine) [16] and could be attributed to the higher oxidation state of rhenium atom (+1) than tungsten (0), which greatly raises the energy separation between metal d orbitals and pyridyl π^* orbitals. In accordance with this argument, the influence of ancillary ligands and substituents of pyridines on the metal to π^* (pyridine) charge-transfer bands is found to be smaller for the above new complexes than for tungsten analogues. It is peculiar that complexes with APPA ligands have MLCT bands of longer wavelength than those with NPPA ligands (i.e. **4** vs. **3**, **11** vs. **10**). We suspect that the rhenium fragment in **4** or **11** actually acts as an induc-

[a] Measured in CH_2Cl_2 solution. [b] Measured in acetone-d_6 except for **2**, **3**, and **5**, which were measured in $CDCl_3$. [c] Reported in ppm relative to $\delta(Me_4Si)$ 0 ppm. [d] Reported in ppm relative to δ (85% H_3PO_4) 0 ppm. [e] The signals due to the AA′MM′ spin system in symmetrical Cp ligands are, due to their simple appearance, reported as triplets with coupling constants equal to half of the separation between the two outer lines. Abbreviations: s = singlet, d = doublet, hept = heptet, quint = quintet, t = triplet, m = multiplet.

Table 5
IR spectra in the ν(CO) region and ^{1}H and ^{31}P{H} NMR spectra of compounds

Compound	ν(CO), (ν(C≡C)) [a] (cm^{-1})	^{1}H δ (ppm) [b,c], J (Hz)	^{31}P{H} δ (ppm) [b,d], J (Hz)
1	2027 vs, 1925 s, 1891 s	NC*H* (8.91, d, 2H, ^3J(H–H) = 6.8); NC*H* (8.68, d, 2 H, ^3J(H–H) = 6.0); NCHC*H* (7.72, d, 2H, ^3J(H–H) = 6.8); NCHC*H* (7.54, d, 2 H, ^3J(H–H) = 6.0)	
2	2026 vs, 1925 s, 1892 m	NC*H* (8.70, d, 4 H, ^3J(H–H) = 6.7); NCHC*H* (7.28, d, 4 H, ^3J(H–H) = 6.7); C*H* (4.55, s, 4 H); C*H* (4.35, s, 4 H); C_5H_5 (4.24, s, 10 H)	
3	2028 vs, 1929 s, 1892 m	NC*H* (8.84, d, 2 H, ^3J(H–H) = 6.8); NC*H* (8.25, d, 2 H, ^3J(H–H) = 8.9); NCHC*H* (7.71, d, 2 H, ^3J(H–H) = 8.9); NCHC*H* (7.41, d, 2 H, ^3J(H–H) = 6.8)	
4	2026 vs, 1925 s, 1891 m	NC*H* (8.78, d, 2 H, ^3J(H–H) = 6.1); NCHC*H* (7.51, d, 2 H, ^3J(H–H) = 6.1); C*H*CNH_2 (7.32, d, 2 H, ^3J(H–H) = 8.2); C*H*CHCNH_2 (6.70, d, 2 H, ^3J(H–H) = 8.2); NH_2 (5.31, s, 2 H)	
5	2031 vs, 1938 s, 1893 s	NC*H* (8.74, d, 4 H, ^3J(H–H) = 6.8); C_6H_4 (7.58, s, 4 H); P*Ph*$_3$ (7.48–7.27, m, 30 H); NCHC*H* (7.04, d, 4 H, ^3J(H–H) = 6.8)	*P* (17.5, s)
6	2032 vs, 1938 s, 1892 s	NC*H* (8.92, d, 4 H, ^3J(H–H) = 6.9); P*Ph*$_3$ and NCHC*H* (7.56–7.34, m, 34 H)	*P* (21.5, s)
7	2040 vs, 1951 s, 1902 s	NC*H* (9.26, d, 4 H, ^3J(H–H) = 6.6); NCHC*H* (7.78, d, 4 H, ^3J(H–H) = 6.6); *Me* (3.73, d, 18 H, ^3J(H–H) = 23.4)	*P* (126, s)
8	2031 vs, 1938 s, 1893 s	NC*H* (8.90, d, 2 H, ^3J(H–H) = 6.8); C*H*CNO_2 (8.32, d, 2 H, ^3J(H–H) = 8.7); C*H*CHCNO_2 (7.91, d, 2 H, ^3J(H–H) = 8.7); P*Ph*$_3$ and NCHC*H* (7.93–7.38, m, 32 H)	*P* (21.1, s)
9 [e]	2030 vs, 1934 s, 1890 s, (2205 *w*)	NC*H* (8.77, d, 2 H, ^3J(H–H) = 6.7); P*Ph*$_3$ (7.60–7.30, m, 15 H); NCHC*H* (7.23, d, 2 H, ^3J(H–H) = 6.7); C_5H_4 (4.62, t, 2 H, ^3J(H–H) = 1.8); C_5H_4 (4.42, t, 2 H, ^3J(H–H) = 1.8); *Cp* (4.29, s, 5 H)	*P* (20.7, s)
10	2036 vs, 1929 s	*bipy*-6,6′ (9.48, d, 2 H, ^3J(H–H) = 7.3); *bipy*-3,3′ (8.74, d, 2 H, ^3J(H–H) = 7.8); NC*H* (8.62, d 2 H, ^3J(H–H) = 6.6); C*H*CNO_2 (8.29, d, 2 H, ^3J(H–H) = 8.7); *bipy* = 5,5′ (8.01, dt, 2 H, J(H–H) = 7.3; 1.1); C*H*CHCNO_2 (7.83, d, 2 H, ^3J(H–H) = 8.7), NCHC*H* (7.60, d, 2 H, ^3J(H–H) = 6.6)	*P* (−138, hept, ^1J(P–F) = 696)
11	2032 vs, 1925 s	*bipy*-6,6′ (9.46, d, 2 H, ^3J(H–H) = 7.4); *bipy*-3,3 (8.72, d, 2 H, ^3J(H–H) = 8.0); *bipy*-4,4′ (8.48, d, 2 H, ^3J(H–H) = 8.0); NC*H* (8.44, d, 2 H, ^3J(H–H) = 6.6); *bipy*-5,5′ (8.00, dt, 2 H, J(H–H) = 7.4; 1.1); NCHC*H* (7.35, d, 2 H, ^3J(H–H) = 6.6); C*H*CNH_2 (7.23, d, 2 H, ^3J(H–H) = 8.6); C*H*CHCNH_2 (6.66, d, 2 H, ^3J(H–H) = 8.6); NH_2 (5.34, s, 2 H)	*P* (−138, hept, ^1J(P–F) = 696)
12 [e]	2036 vs, 1935 s, (2204 *m*)	*bipy*-6,6′ (9.46, d, 2 H, ^3J(H–H) = 7.4); *bipy*-3,3′ (8.72, d, 2 H, ^3J(H–H) = 6.5); *bipy*-4,4′ (8.48, dt, 2 H, J(H–H) = 6.5; 1.2); NC*H* (8.45, d, 2 H, ^3J(H–H) = 6.8); *bipy*-5,5′ (7.99, dt, 2 H, J(H–H) = 7.4; 1.9); NCHC*H* (7.39, d, 2 H, ^3J(H–H) = 6.8); C_5H_4 (4.55, t, 2 H, ^3J(H–H) = 1.8); C_5H_4 (4.40, t, 2 H, ^3J(H–H) = 1.8), C_5H_5 (4.22, s, 5 H)	*P* (−138, hept, ^1J(P–F) = 696)
13	2036 vs, 1933 s	*bipy*-6,6′ (9.44, d, 2 H, ^3J(H–H) = 7.3); *bipy*-3,3′ (8.71, d, 2 H, ^3J(H–H) = 7.7); NC*H* (8.61, d, 2 H, ^3J(H–H) = 6.8); *bipy*-4,4′ (8.45, dt, 2 H, J(H–H) = 7.7; 1.4); *bipy*-5,5′ (7.98, dt, 2 H, J(H–H) = 7.3; 1.1); NCHC*H* (7.56, d, 2 H, ^3J(H–H) = 6.8)	*P* (−138, hept, ^1J(P–F) = 696)
14	2036 vs, 1930 s, (2243 *w*)	*bipy*-6,6′ (9.46, d, 2 H, ^3J(H–H) = 7.3); *bipy*-3,3′ (8.72, d, 2 H, ^3J(H–H) = 7.9); NC*H* (8.56, d, 2 H, ^3J(H–H) = 6.7); *bipy*-4,4′ (8.47, dt, 2 H, J(H–H) = 7.9; 1.5); *bipy*-5,5′ (7.99, dt, 2 H, J(H–H) = 7.3; 1.3); NCHC*H* (7.52, d, 2 H, ^3J(H–H) = 6.7)	*P* (−139, hept, ^1J(P–F) = 696)

Table 6
UV spectra (MLCT) [a] and redox potentials [b] for complexes at 298 K

Complex	λ_{max}, CH_2Cl_2	λ_{max} CH_3CN	E_{ox} (ΔE_p)/Re(+1/+2)	E_{red} (ΔE_p)/PY(0/−1); PY(−1/−2)*
1	345 (sh)	not soluble	+1.09 (*i*)	−1.79 (*i*); −2.11 (140)
2	327	323	+0.20(67) [c], +1.05 (*i*), +1.28 (i)	−2.18 (113); −2.41 (107)
3	345 (sh)	not soluble		
4	370	370	+0.56 (i) [d], 1.01 (*i*), 1.33 (i)	−2.23 (*i*); −2.39 (153)
5	350	345	+1.10 (*i*)	−1.87 (59); −2.02 (*i*)*
6	353	342	+1.11 (*i*)	−1.63 (98); −1.92 (120)*
7	344	337	+1.12 (*i*), 1.52 (i)	−1.61 (83); −1.88 (140)*
8	340 (sh)	326	+1.10 (*i*)	−1.40 (88) [e], −1.79 (78)*
9	326	322	+0.20(93) [c], +1.06 (*i*)	−2.36 (*i*)
10	340 (sh)	330 (sh)	+1.33(104)	−1.38 (68) [e], −1.62 (71) [f], −1.75 (*i*), −2.07 (i) [e]
11	380 [g]	374 [g]	+0.59 (i) [d], 1.39 (*i*)	−1.62 (116) [f], −1.83 (80) [h], −2.12 (*i*)
12	340 (sh)	330 (sh)	+0.16 (64) [c], +1.35 (*i*)	−1.63 (121) [f], −1.85 (i) [h], −2.13 (*i*)
13	349	340	+1.38 (100)	−1.37 (i), −1.56 (i) [f], −1.70(*i*)
14	354	345	+1.40 (86)	−1.60 (i) [f], −2.09 (*i*)
DPB				−2.22 (i), −2.37 (i)
BPEB				−2.39 (i)
FPA				> −2.89
NPPA				−1.42 (100), −2.12 (205)
APPA			+1.09 (i)	−1.43 (i), −2.01 (i), −2.21 (i)

[a] MLCT = rhenium dπ to pyridine π^* charge transfer; the λ_{max} values are in units of nm. [b] Analyses performed in 10^{-3} M deoxygenated CH_2Cl_2 (**1–9**) or CH_3CN (**10–14**) solutions containing 0.1 M TBAP, scan rate is 80 mV s^{-1} (CH_2Cl_2) or 100 mV s^{-1} (CH_3CN). All potentials in volts vs. ferrocene (0.00 V with peak separation of 105 mV in CH_2Cl_2 and 77 mV in CH_3CN); scan range +1.5 to −2.5 V; (i) = irreversible process; $\Delta E_P = E_{pa} - E_{pc}$ (mV). [c] E_{ox}(Fe(+2/+3)). [d] Oxidation of NH_2. [e] Reduction of NO_2. [f] E_{red} (bipy(0/−1)). [g] The MLCT band is assigned as the rhenium dπ to bipy π^* charge transfer. [h] E_{red} (bipy(−1/−2)).

tive acceptor, similar to those reported by Marks and coworkers [5a] and Zyss and coworkers [5b].

Redox potential values obtained from cyclic voltammetry data of the compounds in this study are also listed in Table 6. It was known that Re(bipy)$(CO)_3$Cl decomposed in CH_3CN upon oxidation or reduction [17]; therefore, electrochemical measurements for **1–9** were performed in CH_2Cl_2. It should be more difficult to remove an electron from an Re(I) than from a W(0) atom of the same electronic configuration [18], and the oxidation potentials of Re atoms in **1–14** are indeed significantly more positive (greater than 300 mV) than those in $W(CO)_4(L)(PY)$ and $[W(CO)_4(L)]_2(\mu\text{-PY}')$. Cationic complexes, **10–14**, also have higher E_{OX} than those of **1–9**, as expected.

Reduction potentials for PY π^* levels of the complexes are consistent with the energy stabilization of π^*-acceptor orbital upon ligation of PY. The two re-

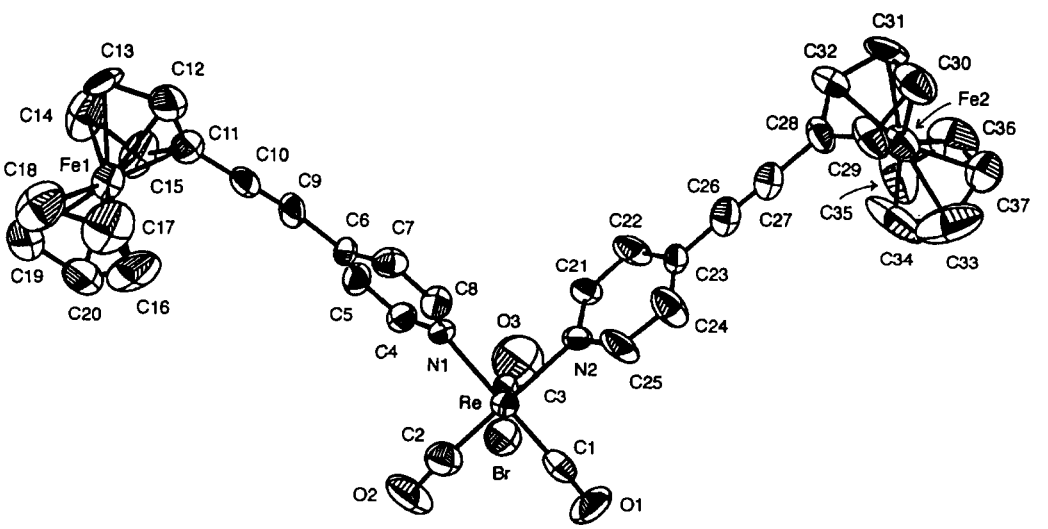

Fig. 1. ORTEP drawing of **2**. Thermal ellipsoids are drawn with 30% probability boundaries.

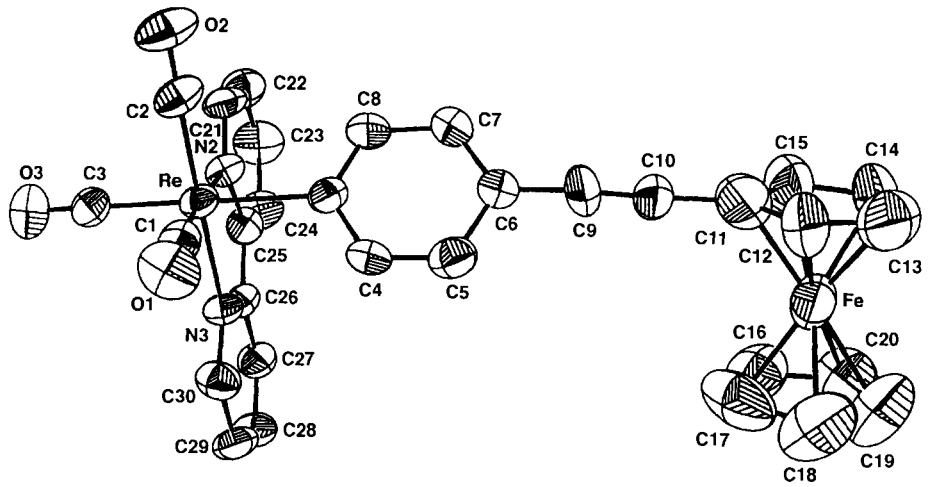

Fig. 2. ORTEP drawing of $[12]^+$. Thermal ellipsoids are drawn with 30% probability boundaries.

duction potentials for **2** and **4** (Table 6) are more likely to be due to the one-electron reduction of the first PY and the second PY ligands respectively, instead of the one-electron reduction and the second electron reduction on the same PY ligand, since the latter is expected to be energetically less favored [19]. The presence of two reduction potentials in **2** and **4** also implies that the π^* orbitals of two PY ligands are mutually affected through the metal. An electron-withdrawing substituent evidently shifts the PY π^*-acceptor orbital to a lower energy and an electron-donating substituent does the opposite (e.g. **8** vs. **9** and **10** vs. **11**). The potential difference between the oxidation and the first reduction potentials, $E_{ox} - E_{red}(0/1-)$, is also in agreement with the larger MLCT transition energy for aforementioned rhenium complexes (2.70–3.48 eV) than for $W(CO)_4(L)(PY)$ and $[W(CO)_4(L)]_2(\mu\text{-PY})$ (1.69–2.94 eV).

The molecular structures of $\mathbf{2} \cdot CH_2Cl_2$ and $\mathbf{12} \cdot 2H_2O$ were established by X-ray diffraction analysis. The ORTEP drawings of **2** and $[\mathbf{12}]^+$ are shown in Figs. 1 and 2. The rhenium atom resides in an approximately octahedral environment with the facial disposition for the three carbonyl ligands. The Re–C–O linkage (176(2)–178(2)°) does not deviate significantely from linearity except for Re–C3–O3/Re–C3′–O3′ (153.62/163.12 Å) of **2** owing to the disordered carbonyl ligand. The carbonyl Re–C distances range from 1.86 to 2.01 Å. Other relevant crystal data also appear to be normal: the alkynyl C≡C distances range from 1.13(2) to 1.20(2) Å. The Re–N distances (2.14(1)–2.252(5) Å) are comparable with literature values [20].

In summary, we synthesized rhenium carbonyls containing ethynyl pyridyl ligands. As a complement to our previous study [2], we also demonstrated that variation of metal atoms could potentially provide an efficient way to tune molecules for electron transfer and nonlinear optical applications.

4. Supplementary materials available

Complete crystal data, all bond distances and angles, positional parameters, anisotropic thermal parameters and isotropic thermal parameters, and a table of rhenium-to-PY charge transfer absorption maxima for all complexes in different solvents, electronic spectra of **3**, **8**, and **10**, a plot of rhenium-to-PY charge transfer absorption maxima of **5**–**9** against solvent parameter, cyclic voltammograms of **10** and **8**, and stereoviews for complexes $\mathbf{2} \cdot CH_2Cl_2$ and $\mathbf{12} \cdot 2H_2O$ (21 pages), are available from the authors.

Acknowledgement

We thank the National Science Foundation of the Republic of China for financial support (Grants NSC-84-2113-M-001-017).

References

[1] N.J. Long, *Angew. Chem. Int. Ed. Engl.*, *34* (1995) 21.
[2] J.T. Lin, S.S. Sun, J.J. Wu, L.S. Lee, K.J. Lin and Y.F. Huang, *Inorg. Chem.*, *34* (1995) 2323.
[3] (a) D.R. Kanis, M.A. Ratner and T.J. Marks, *Chem. Rev.*, *94* (1994) 195; (b) M. Bourgault, W. Tam and D.F. Eaton, *Organometallics*, *9* (1990) 2856.
[4] G.L. Geoffroy and M.S. Wrighton (eds.), *Organometallic Photochemistry*, Academic Press, New York, 1979.
[5] (a) D.R. Kanis, P.G. Lacroix, M.A. Ratner and T.J. Marks, *J. Am. Chem. Soc.*, *116* (1994) 10089; (b) M. Bourgault, C. Mountassir, H.Le. Bozec, I. Ledoux, G. Pucetti and J. Zyss, *J. Chem. Soc. Chem. Commun.*, (1993) 1623.
[6] (a) U.H.F. Bunz, V. Enkelmann and J. Räder, *Organometallics*, *12* (1993) 4745; (b) J.E.C. Wiegelmann and U.H.F. Bunz, *Organometallics*, *12* (1993) 3792; (c) C.L. Sterzo and J.K. Stille, *Organometallics*, *9* (1990) 687; (d) C.L. Sterzo, M.M. Miller and J.K. Stille, *Organometallics*, *8* (1989) 2331.

[7] (a) G. Jia, R.J. Puddephatt, J.J. Vittal and N.C. Payne, *Organometallics, 12* (1993) 263; (b) M. Zeldih, K. Wynne and H.R. Allcock (eds.), *Inorganic and Organometallic Polymers, Advances in Chemistry Series 224*, American Chemical Society, Washington, DC, 1988.

[8] (a) E.E. Bunel, L. Valle, N.L. Jones, P.J. Carroll, M. Gonzalez, N. Munoz, and J.M. Manriquez, *Organometallics, 7* (1988) 789; (b) V. Grosshenny and R. Ziessel, *J. Chem. Soc. Dalton Trans.*, (1993) 817; (c) A. Das, J.P. Maher, J.A. McCleverty, J.A.N. Badiola and M.D. Ward, *J. Chem. Soc. Dalton Trans.*, (1993) 681; (d) K.T. Potts, C.P. Horwitz, A. Fessak, K.M. Keshararz, K.E. Nash and P.J. Toscano, *J. Am. Chem. Soc., 15* (1993) 10444; (e) J.E. Sutton and H. Taube, *Inorg. Chem., 20* (1981) 3125.

[9] R.B. King (ed.), *Organometallic Synthesis, Transition-Metal Compounds*, Vol. 1, Academic Press, New York, 1965.

[10] F. Zingales, U. Sartorelli, F. Canziani and M. Raveglia, *Inorg. Chem., 6* (1967) 154.

[11] J.V. Caspar and T.J. Meyer, *J. Phys. Chem., 87* (1983) 952.

[12] E.J. Gabe, Y. LePage, J.P. Charland, F.L. Lee and P.S. White, *J. Appl. Crystallogr., 22* (1989) 384.

[13] P. Main, S.J. Fiske, S.E. Hull, L. Lessinger, G. Germain, J.P. Declercq and M.M. Woolfson, MULTAN80 *A system of computer programs for the automatic solution of crystal structures from X-ray diffraction data*, 1980 (Universities of York, UK and Louvain, Belgium).

[14] (a) G. Wilkinson, F.G.A. Stone and E.W. Abel (eds.), *Comprehensive Organometallic Chemistry*, Vol. 4, Pergamon, Oxford, UK, 1982, Chapter 30; (b) R.H. Reimann and E. Singleton, *J. Organomet. Chem.*, (1973) 309; (c) F. Zingales, U. Sartorelli and A. Trovati, *Inorg. Chem., 6* (1967) 1246.

[15] (a) W. Kaim and S. Kohlmann, *Inorg. Chem., 25* (1986) 3306; (b) D.M. Manuta and A.J. Lees, *Inorg. Chem., 22* (1983) 3825; (c) W. Kaim, S. Kuhlmann, S. Ernst, B. Olbrich-Deussner, C. Bessenbacher and A. Schulz, *J. Organomet. Chem., 321* (1987) 215.

[16] P.J. Giordano and M.S. Wrighton, *J. Am. Chem. Soc., 101* (1979) 2888.

[17] (a) J.K. Hino, L.D. Ciana, W.J. Dressick and B.P. Sullivan, *Inorg. Chem., 31* (1992) 1072; (b) A.I. Breikss and H.D. Abruna, *J. Eletroanal. Chem., 201* (1986) 347.

[18] M.M. Zulu and A.J. Lees, *Organometallics, 8* (1989) 955.

[19] M.M. Zulu and A.J. Lees, *Inorg. Chem., 27* (1986) 1139.

[20] P.C. Chen, M. Curry and T.J. Meyer, *Inorg. Chem., 28* (1989) 2271.